THE JOURNAL OF PHYSICAL CHEMISTRY B

Article

pubs.acs.org/JPCB

Membrane Organization and Dynamics of "Inner Pair" and "Outer Pair" Tryptophan Residues in Gramicidin Channels

Sourav Haldar,[†] Arunima Chaudhuri,[†] Hong Gu,[‡] Roger E. Koeppe, II,[‡] Mamata Kombrabail,[§] G. Krishnamoorthy,[§] and Amitabha Chattopadhyay*,[†]

[†]Centre for Cellular and Molecular Biology, Council of Scientific and Industrial Research, Uppal Road, Hyderabad 500 007, India

[‡]Department of Chemistry and Biochemistry, University of Arkansas, Fayetteville, Arkansas 72701, United States

[§]Department of Chemical Sciences, Tata Institute of Fundamental Research, Homi Bhabha Road, Mumbai 400 005, India

ABSTRACT: The linear ion channel peptide gramicidin serves as an excellent prototype for monitoring the organization, dynamics, and function of membrane-spanning channels. The tryptophan residues in gramicidin channels are crucial for establishing and maintaining the structure and function of the channel in the membrane bilayer. In order to address the basis of differential importance of tryptophan residues in the gramicidin channel, we monitored the effects of pairwise substitution of two of the four gramicidin tryptophans, the inner pair (Trp-9 and -11) and the outer pair (Trp-13 and -15), using a combination of steady state and time-resolved fluorescence approaches and circular dichroism spectroscopy. We show here that these double tryptophan gramicidin analogues adopt different conformations in membranes, suggesting that the conformational preference of double tryptophan gramicidin analogues is dictated by the positions of the tryptophans in the sequence. These results assume significance in the context of recent observations that the inner pair of tryptophans (Trp-9 and -11) is more important for gramicidin channel formation and channel conductance. These results could be potentially useful in analyzing the effect of tryptophan substitution on the functioning of ion channels and membrane proteins.

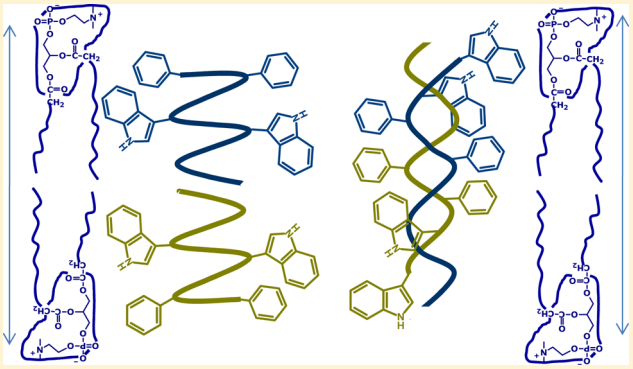

INTRODUCTION

Cellular membranes are complex two-dimensional, anisotropic assemblies of a diverse variety of lipids and proteins. Membrane proteins mediate a wide range of essential cellular processes such as signaling, cell−cell recognition, and membrane transport. About 30% of open reading frames (ORFs) are predicted to encode membrane proteins.[1,2] Importantly, they represent prime candidates for the generation of novel drugs in all clinical areas[3,4] owing to their involvement in a variety of cellular processes. However, membrane proteins are difficult to crystallize in their native conditions due to the intrinsic dependence on surrounding membrane lipids.[5] It is in this context that approaches based on fluorescence spectroscopy have proved useful in elucidating the organization, topology, and orientation of membrane proteins and peptides.[6−8] An advantage of spectroscopic approaches is that the information obtained is dynamic in nature, necessary for understanding membrane protein function. The presence of tryptophan residues as intrinsic fluorophores in membrane peptides and proteins makes them an attractive choice for fluorescence spectroscopic analyses.[6,8,9] Interestingly, integral membrane proteins are reported to have a significantly higher tryptophan content than soluble proteins.[10]

The linear peptide gramicidin forms ion channels specific for monovalent cations and has been extensively used to monitor the organization, dynamics, and function of membrane-spanning channels and integral membrane proteins.[11] Gramicidin represents an excellent prototype for monitoring membrane protein conformation and dynamics due to its small size, ready availability, and relative ease with which chemical modifications can be performed.[12] These features make gramicidin unique among small membrane-active peptides and provide the basis for its use to explore the principles that govern the folding and function of membrane-spanning channels in particular, and membrane proteins in general.[11−13] In spite of the alternating sequence of L−D chirality (see Figure 1), gramicidin represents a useful model for realistic determination of conformational preference of proteins in a membrane environment. This is due to the fact that the dihedral angle combinations generated in the conformation space by various gramicidin conformations are allowed according to the Ramachandran plot.[14] In addition, gramicidin channels share crucial structural features involving ion selectivity with complex ion channels such as KcsA potassium channels.[15]

Received: May 18, 2012
Revised: July 18, 2012
Published: August 14, 2012

   dx.doi.org/10.1021/jp304846f | J. Phys. Chem. B 2012, 116, 11056−11064

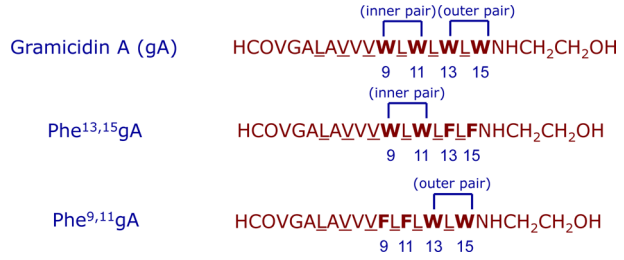

Figure 1. Amino acid sequence of gramicidin A and the double tryptophan analogues used. Alternating D-amino acid residues are underlined. Aromatic amino acids are highlighted and their positions shown. Tryptophan residues at positions 9 and 11 are designated as the "inner pair", while tryptophan residues at positions 13 and 15 are designated as the "outer pair". The analogue in which the inner pair of tryptophans are substituted by phenylalanine is denoted as Phe^{9,11}gA, while the analogue in which the outer pair of tryptophans are substituted is termed Phe^{13,15}gA.

Gramicidin has been shown to assume two major folding motifs in various media: (i) the single stranded helical dimer ("channel" form) and (ii) the double stranded intertwined helix (collectively known as the "nonchannel" form).[12] The single stranded helical dimer conformation is the thermodynamically preferred conformation in membranes and membrane-mimetic environments.[16−19] The cation conducting gramicidin channel in membranes is formed by the head-to-head (amino terminal-to-amino terminal) single stranded $\beta^{6.3}$ helical dimer.[20] In this conformation, the carboxy terminus is exposed to the membrane−water interface and the amino terminus is buried in the hydrophobic core of the membrane. This conformation involves a clustering of the tryptophan residues at the membrane−water interface around the entrance to the channel.[17,20−22] Indeed, the interfacial localization of the gramicidin tryptophan residues is an essential aspect of gramicidin conformation and function in membranes.[11,23] The membrane interface seeking properties of tryptophan[24−26] and the oriented dipole moments of the tryptophan side chains play an important role in gramicidin conformation and ion channel activity,[12] a feature shared by other membrane proteins.[23] Interestingly, the membrane interfacial localization of tryptophan residues is absent in "nonchannel" conformations and the tryptophan residues are distributed along the membrane axis.[12,17,23] Such nonchannel conformations have been shown to exist in membranes with polyunsaturated lipids,[27] and in membranes with increased acyl chain lengths under hydrophobic mismatch conditions.[28,29]

Among ion channels, gramicidin represents a particularly powerful model for clarifying the importance of tryptophan at the membrane−water interface for channel structure and assembly.[30−36] The tryptophan residues in gramicidin channels are crucial for maintaining the structure and function of the channel.[30−37] It has been shown previously that gramicidins with Trp → Phe substitutions have greater difficulty in forming membrane-spanning dimeric channels.[31,35] The parent peptide gramicidin A (gA) has the sequence shown in Figure 1. The peptide has four tryptophans at positions 9, 11, 13, and 15. Interestingly, it has recently been suggested that Trp-9 and Trp-11 (denoted as "inner pair" Trp's; see Figure 1) are more important in maintaining gramicidin channel structure and function than Trp-13 and Trp-15 (the "outer pair'").[37,38]

In order to characterize this aspect further and to address the molecular basis of differential importance of tryptophan residues in gramicidin channels, we explored the organization and dynamics of double tryptophan (pairwise Trp → Phe substituted) analogues of gramicidin in membranes (Figure 1). Toward this goal, we applied a combination of fluorescence approaches which include red edge excitation shift (REES), membrane penetration depth, fluorescence lifetime distribution, and fluorescence anisotropy decay, along with circular dichroism (CD) spectroscopy. Our results show that the organization and dynamics of the inner and outer pairs of tryptophan residues in gramicidin differ and are dependent on their localization along the bilayer normal. These results correlate well with recent single-channel and solid-state NMR results of gramicidin channels in which the inner or outer pair of tryptophan residues has been either methylated[37] or replaced with phenylalanine.[38]

EXPERIMENTAL SECTION

Materials. 1-Palmitoyl-2-oleoyl-*sn*-glycero-3-phosphocholine (POPC), 1,2-dioleoyl-*sn*-glycero-3-phosphocholine (DOPC), 1-palmitoyl-2-(5-doxyl)stearoyl-*sn*-glycero-3-phosphocholine (5-PC), and 1-palmitoyl-2-(12-doxyl)stearoyl-*sn*-glycero-3-phosphocholine (12-PC) were obtained from Avanti Polar Lipids (Alabaster, AL). 2-(9-Anthroyloxy)stearic acid (2-AS) and 12-(9-anthroyloxy)stearic acid (12-AS) were from Molecular Probes (Eugene, OR). 1,2-Dimyristoyl-*sn*-glycero-3-phosphocholine (DMPC) was purchased from Sigma Chemical (St. Louis, MO). The double tryptophan analogues of gramicidin were synthesized using methods described earlier.[38] The concentration of double tryptophan gramicidin analogues was estimated from a molar extinction coefficient of 11 000 M^{-1} cm^{-1} at 280 nm. Lipids were checked for purity by thin layer chromatography on silica gel precoated plates (Sigma) in chloroform/methanol/water (65:35:5, v/v/v) and were found to give only one spot in all cases with a phosphate-sensitive spray and subsequent charring.[39] The concentration of phospholipids was determined by phosphate assay subsequent to total digestion by perchloric acid.[40] DMPC was used as an internal standard to assess lipid digestion. All other chemicals used were of the highest purity available. Solvents used were of spectroscopic grade. Water was purified through a Millipore (Bedford, MA) Milli-Q system and used for all experiments.

Sample Preparation. Experiments were performed using small unilamellar vesicles (SUV) of POPC containing 2% (mol/mol) gramicidin analogue. In general, 1280 nmol of POPC in chloroform/methanol was mixed with 25.6 nmol of the gramicidin analogue in methanol. A few drops of chloroform were added to this solution. The solution was mixed well and dried under a stream of nitrogen while warming gently (~40 °C) and dried further under a high vacuum for at least 12 h. The dried film was swelled in 1.5 mL of 10 mM sodium phosphate, 150 mM sodium chloride, pH 7.2 buffer, and samples were vortexed for 3 min to uniformly disperse lipids and peptide. The samples were sonicated to clarity under argon (~30 min in short bursts while being cooled in an ice/water mixture) using a Branson model 250 sonifier (Branson Ultrasonics, Dansbury, CT) fitted with a microtip. The sonicated samples were centrifuged at 15 000 rpm in a Heraeus Biofuge (DJB Labcare, Buckinghamshire, U.K.) for 15 min to remove any titanium particles shed from the microtip during sonication and incubated for 12 h at 65 °C with continuous shaking. Samples were incubated in the dark at room temperature (~25 °C) for 1 h before fluorescence or CD measurements. Background samples were prepared the same

way except that the gramicidin analogue was omitted. All experiments were done with multiple sets of samples at room temperature (~25 °C).

Depth Measurements Using the Parallax Method. The actual spin (nitroxide) content of spin-labeled phospholipids (5- and 12-PC) was assayed using fluorescence quenching of anthroyloxy-labeled fatty acids (2- and 12-AS) as described earlier.[41] For depth measurements, SUVs were prepared by sonication followed by incubation at 65 °C for 12 h as described above. These samples were made by drying 160 nmol of DOPC containing 15 mol % spin-labeled phospholipid (5- or 12-PC) and 3.2 nmol of gramicidin analogue under a stream of nitrogen while being warmed gently (~35 °C) and then kept under a high vacuum for at least 3 h. Duplicate samples were prepared in each case except for samples lacking the quencher (5- or 12-PC) where triplicates were prepared. Background samples lacking the fluorophore (gramicidin analogue) were prepared in all experiments, and their fluorescence intensity was subtracted from the respective sample fluorescence intensity.

Steady State Fluorescence Measurements. Steady state fluorescence measurements were performed with a Hitachi F-4010 steady state spectrofluorometer (Tokyo, Japan) using 1 cm path length quartz cuvettes. Excitation and emission slits with a nominal bandpass of 5 nm were used. Background intensities of samples in which the fluorophore was omitted were subtracted from each sample spectrum to cancel out any contribution due to the solvent Raman peak and other scattering artifacts. The spectral shifts obtained with different sets of samples were identical in most cases. In other cases, the values were within ±1 nm of those reported.

Circular Dichroism Measurements. CD measurements were carried out at room temperature (~25 °C) on a JASCO J-815 spectropolarimeter (Tokyo, Japan) which was calibrated with (+)-10-camphorsulfonic acid. The spectra were scanned in a quartz optical cell with a path length of 0.1 cm. All spectra were recorded in 0.5 nm wavelength increments with a 4 s response and a bandwidth of 1 nm. For monitoring changes in secondary structure, spectra were scanned in the far-UV range from 200 to 260 nm at a scan rate of 100 nm/min. Each spectrum is the average of 12 scans with a full scale sensitivity of 10 mdeg. All spectra were corrected for background by subtraction of appropriate blanks. Data are represented as mean residue ellipticities and were calculated using the formula

$$[\theta] = \theta_{obs}/(10Cl) \tag{1}$$

where θ_{obs} is the observed ellipticity in mdeg, l is the path length in cm, and C is the concentration of peptide bonds in mol/L.

Time-Resolved Fluorescence Measurements. Time-resolved fluorescence intensity decay measurements were carried out using a time correlated single photon counting (TCSPC) setup. For fluorescence lifetime measurements, 1 ps pulses of 887 nm radiation from the Ti-sapphire femto/picosecond laser (Spectra Physics, Mountain View, CA), pumped by an Nd−YLF laser (Millenia X, Spectra Physics), were frequency tripled to 295 nm by using a frequency doubler/tripler (GWU, Spectra physics). Fluorescence decay curves were obtained at a laser repetition rate of 4 MHz by a microchannel plate photomultiplier (model R2809u, Hamamatsu Corp.) coupled to a TCSPC setup. The instrument response function (IRF) at 295 nm was obtained using a dilute colloidal suspension of dried nondairy creamer. The full width at half maxima (fwhm) of the IRF was 40 ps, and the number of channels used was 1024. Fluorescence emission measurements of gramicidin, excited at 295 nm, were carried out at 340 nm, using a combination of a monochromator and a 320 nm cutoff filter. Fluorescence intensity decay was collected from samples after excitation with the emission polarizer oriented at the magic angle (54.7°) with respect to the excitation polarizer. Fluorescence emission at magic angle (54.7°) was dispersed in a monochromator (spectral width 2.5 nm) and counted ((3−4) × 10^3 s^{-1}) by a microchannel plate photomultiplier, processed through a constant fraction discriminator, time-to-amplitude converter, and multichannel analyzer. To optimize the signal-to-noise ratio, 20 000 photon counts were collected in the peak channel. All experiments were performed using excitation and emission slits with a nominal bandpass of 3 nm or less. The data stored in the multichannel analyzer was routinely transferred to an IBM PC for analysis. Fluorescence intensity decay curves so obtained were deconvoluted with the instrument response function and analyzed as a sum of exponential terms:

$$F(t) = \sum_i \alpha_i \exp(-t/\tau_i) \tag{2}$$

where $F(t)$ is the fluorescence intensity at time t and α_i is a pre-exponential factor representing the fractional contribution to the time-resolved decay of the component with a lifetime τ_i such that $\sum\alpha_i = 1$. The decay parameters were recovered using a nonlinear least-squares iterative fitting procedure based on the Levenberg−Marquardt algorithm. A fit was considered acceptable when plots of the weighted residuals and the autocorrelation function showed random deviation about zero with a minimum χ^2 value not more than 1.2. Amplitude-averaged lifetimes (τ_m) and intensity-averaged lifetimes ($\langle\tau\rangle$) for triexponential decays of fluorescence were calculated from the decay times and pre-exponential factors using the following equations:[42,43]

$$\tau_m = \alpha_1\tau_1 + \alpha_2\tau_2 + \alpha_3\tau_3 \tag{3}$$

$$\langle\tau\rangle = \frac{\alpha_1\tau_1^2 + \alpha_2\tau_2^2 + \alpha_3\tau_3^2}{\alpha_1\tau_1 + \alpha_2\tau_2 + \alpha_3\tau_3} \tag{4}$$

Fluorescence decays were further analyzed by fluorescence lifetime distribution analysis using the maximum entropy method (MEM). Analysis of fluorescence lifetime data by MEM is bias-free (model independent). Details of lifetime analysis by MEM are described elsewhere.[7,44]

Analysis of Time-Resolved Fluorescence Anisotropy. Time-resolved fluorescence anisotropy was analyzed as described previously.[44,45] The fluorescence intensity decays were collected with the emission polarizer kept at parallel ($I_\parallel$) and perpendicular ($I_\perp$) orientations with respect to the excitation polarizer. Anisotropy was calculated as

$$r(t) = \frac{I_\parallel(t) - GI_\perp(t)}{I_\parallel(t) + 2GI_\perp(t)} \tag{5}$$

where G is the grating factor (G-factor). The G-factor is defined as the ratio of the transmission efficiency of the grating for vertically polarized light to horizontally polarized light. The G-factor of the emission collection optics was determined in a separate experiment using a standard sample (NATA). The time-resolved anisotropy decay was analyzed on the basis of the model:

$$I_{\parallel}(t) = I(t)[1 + 2r(t)]/3 \quad (6)$$

$$I_{\perp}(t) = I(t)[1 - r(t)]/3 \quad (7)$$

where $I_{\parallel}(t)$ and $I_{\perp}(t)$ are the decays of the parallel ($\parallel$) and perpendicular ($\perp$) components of emission. The equation for time-resolved fluorescence anisotropy can be expressed as a triexponential decay:

$$r(t) = r_0\{\beta_1 \exp(-t/\phi_1) + \beta_2 \exp(-t/\phi_2) + \beta_3 \exp(-t/\phi_3)\} \quad (8)$$

where ϕ_i and β_i represent the ith rotational correlation time and the corresponding pre-exponential factor in the exponential anisotropy decay such that $\sum\beta_i = 1$. r_0 represents the anisotropy at zero time (initial anisotropy). The goodness of the fit of a given set of observed data and the chosen function was evaluated by the reduced χ^2 ratio which is around 1.0−1.2.

RESULTS

Fluorescence Characteristics of Double Tryptophan Analogues of Gramicidin. Fluorescence spectroscopy has been previously utilized as a suitable approach in elucidating gramicidin conformations in membranes.[7,17,22,29,36] The sequences of double tryptophan (pairwise Trp → Phe substituted) gramicidin analogues used are shown in Figure 1. We monitored the immediate membrane environment experienced by the inner and outer pairs of tryptophans (other tryptophans being replaced by phenylalanine which is practically nonfluorescent under these conditions) in these analogues when bound to membranes. The fluorescence emission maximum of gramicidin in the channel conformation in POPC membranes is 333 nm, whereas the nonchannel conformation exhibits an emission maximum of 335 nm,[17] when excited at 280 nm. The normalized emission spectra of double tryptophan gramicidin analogues (Phe^{9,11}gA and Phe^{13,15}gA) are shown in Figure 2a. The analogue (Phe^{13,15}gA) containing the inner pair of tryptophans (Trp-9 and -11) displays an emission maximum of 331 nm, while the analogue (Phe^{9,11}gA) containing the outer pair of tryptophans (Trp-13 and -15) displays a red-shifted emission maximum of 338 nm. The difference in fluorescence emission maximum among the analogues is indicative of differential localization of the tryptophans along the membrane axis (see later). This is particularly true for the nonchannel conformation of gramicidin where the tryptophan residues are distributed more evenly along the backbone relative to their distribution in the channel conformation.[17]

A shift in the wavelength of maximum fluorescence emission toward higher wavelengths, caused by a shift in the excitation wavelength toward the red edge of the absorption band, is termed red edge excitation shift (REES).[8,9,46,47] This effect is mostly observed with polar fluorophores in motionally restricted environments such as viscous solutions or condensed phases where the dipolar relaxation time for the solvent shell around a fluorophore is comparable to or longer than its fluorescence lifetime. While other fluorescence techniques yield information about the fluorophore itself, REES provides information about the relative rates of solvent relaxation that is not possible to obtain by other techniques. We have previously shown that REES can be used as a sensitive tool to monitor gramicidin conformations in membranes and membrane-mimetic environments.[17−19,22] The shifts in the maxima

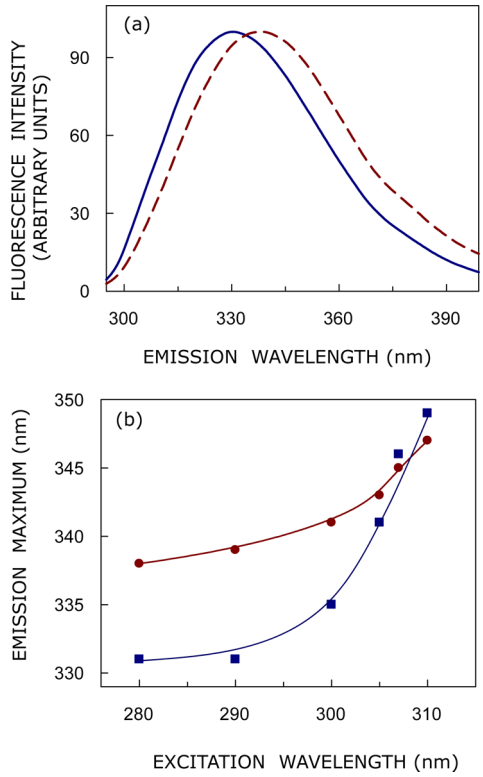

Figure 2. (a) Fluorescence emission spectra of gramicidin analogues in vesicles of POPC. The spectra corresponding to Phe^{13,15}gA (—) and Phe^{9,11}gA (---) are shown. The excitation wavelength was 280 nm in both cases. Spectra are intensity-normalized at the respective emission maximum. (b) Effect of changing excitation wavelength on the wavelength of maximum emission for Phe^{13,15}gA (■) and Phe^{9,11}gA (●). Lines joining data points are provided merely as viewing guides. The ratio of peptide to POPC was 1:50 (mol/mol), and the concentration of POPC was 0.85 mM. See the Experimental Section for more details.

of fluorescence emission of the tryptophan residues of the gramicidin analogues as a function of excitation wavelength are shown in Figure 2b. (We have used the term "maximum of fluorescence emission" in a somewhat wider sense here. In every case, we monitored the wavelength corresponding to maximum fluorescence intensity, as well as the center of mass of the fluorescence emission. In most cases, both of these methods yielded the same wavelength. In cases where minor discrepancies were found, the center of mass of emission has been reported as the fluorescence maximum.) As the excitation wavelength is changed from 280 to 310 nm, the emission maximum is shifted from 338 to 347 nm for the analogue (Phe^{9,11}gA) containing the outer pair of tryptophans (see Figure 2b). This shift corresponds to REES of 9 nm. It is possible that there could be further red shift if excitation is carried out beyond 310 nm. We found it difficult to work in this wavelength range due to low signal/noise ratio and artifacts due to the solvent Raman peak that sometimes remain even after background subtraction. Such dependence of the emission maximum on excitation wavelength is characteristic of REES and implies that the outer pair tryptophans (Trp-13 and -15) are localized in motionally restricted regions. On the other hand, Figure 2b shows that the emission maximum is shifted from 331 to 349 nm for the analogue (Phe^{13,15}gA) containing the inner pair of tryptophans (Trp-9 and -11), as the excitation wavelength is changed from 280 to 310 nm. This shift

dx.doi.org/10.1021/jp304846f | J. Phys. Chem. B 2012, 116, 11056−11064

corresponds to an enhanced REES of 18 nm. Interestingly, we have previously reported that the gramicidin analogue containing only Trp-9 exhibits REES of similar magnitude.[36] Such large magnitudes of REES could be due to ground state conformational heterogeneity.

Conformations of Gramicidin Analogues. The variation in fluorescence parameters among the double tryptophan gramicidin analogues could be indicative of different conformations of these analogues in the membrane. CD spectroscopy has been previously utilized to monitor gramicidin conformations in membranes.[17,36,38] We examined the backbone conformation of the gramicidin analogues using CD spectroscopy in POPC, to complement the spectra previously reported for the analogues in DMPC.[38] The CD spectra of the gramicidin analogues are shown in Figure 3, along with the

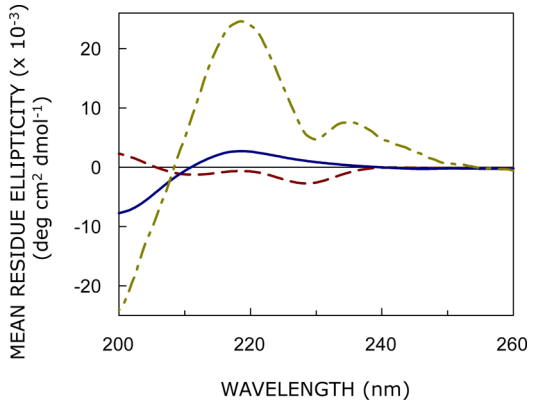

Figure 3. Far-UV CD spectra of gramicidin (–·–), Phe^{13,15}gA (—), and Phe^{9,11}gA (---) in POPC vesicles. The ratio of peptide to POPC was 1:50 (mol/mol), and the concentration of POPC was 0.85 mM. See the Experimental Section for other details.

spectrum for gramicidin in the channel conformation for reference. The characteristic single-stranded $\beta^{6.3}$ channel conformation has typical peaks of positive ellipticity around 218 and 235 nm, a valley around 230 nm, and negative ellipticity below 208 nm. The CD spectra of the gramicidin analogues are varied (Figure 3) and deviate from the spectrum of the channel conformation. Interestingly, the backbone CD spectra of the analogue (Phe^{13,15}gA) with the inner pair of tryptophans (Trp-9 and -11) appears somewhat similar to the channel conformation with relatively low intensity. In contrast, the CD spectrum displayed by the analogue (Phe^{9,11}gA) with the outer pair of tryptophans (Trp-13 and -15) appears comparable to the nonchannel conformation. These results imply that the inner pair of tryptophans are more crucial in maintaining the channel conformation of gramicidin in membranes. Similar results have been reported for the analogues in DMPC,[38] for which it was also demonstrated by size-exclusion chromatography that Phe^{13,15}gA is about 75% in the channel conformation and Phe^{9,11}gA is about 25% in the channel conformation.

Fluorescence Lifetimes of Gramicidin Analogues. Fluorescence lifetime serves as a sensitive indicator of the local environment and polarity in which a given fluorophore is localized.[48] Table 1 shows fluorescence lifetimes of double tryptophan gramicidin analogues analyzed by the discrete analysis method. Fluorescence decays could be fitted well using a triexponential function. The mean amplitude-averaged lifetimes (τ_m) and intensity-averaged lifetimes ($\langle\tau\rangle$) of tryptophans in gramicidin analogues were calculated using eqs 3 and 4 and are shown in Table 1. The average fluorescence lifetimes of the analogue (Phe^{9,11}gA) with the outer pair tryptophans are found to be slightly longer than the analogue (Phe^{13,15}gA) containing the inner pair of tryptophans. Interestingly, tryptophan residues in both analogues exhibit a significantly higher fluorescence lifetime than native gramicidin.[7] A possible reason for the higher fluorescence lifetime in each of these analogues is the release of the aromatic–aromatic interaction between the indole rings of Trp-9 and Trp-15 (also supported by more intense fluorescence of the analogues relative to native gramicidin, when either Trp-9 or Trp-15 is removed). These tryptophan residues have been previously implicated in specific aromatic–aromatic (stacking) interaction in the $\beta^{6.3}$ helical channel form.[22]

Fluorescence decay kinetics in complex systems often display considerable heterogeneity. The fluorescence lifetime distribution in such cases represents a powerful method for characterizing complex heterogeneous systems such as membranes. The width of the lifetime distribution has been used to interpret the integrity and heterogeneity of such systems.[7,44,49] Lifetime distribution analysis by the maximum entropy method (MEM) represents a convenient, robust, and model-free approach of data analysis.[7,44,49] We have previously shown that lifetime distribution using MEM analysis can be conveniently used to monitor the gramicidin conformational heterogeneity in membranes.[7] In MEM analysis, the fluorescence intensity decay is analyzed using the model of continuous distribution of lifetimes. The lifetime distribution profile obtained by the MEM analysis for tryptophans in the gramicidin analogues is shown in Figure 4. The analogue (Phe^{9,11}gA) with the outer pair tryptophans shows a multimodal heterogeneous lifetime distribution profile (Figure 4a), while the analogue (Phe^{13,15}gA) containing the inner pair of tryptophans shows a relatively homogeneous lifetime distribution (Figure 4b). These lifetime distribution profiles were found to be reproducible, indicating that these results are robust. Interestingly, we have previously shown that the lifetime distribution for tryptophan residues of native gramicidin is narrower (more homogeneous) in the channel conformation relative to the corresponding distribution in the nonchannel conformation.[7]

Membrane Penetration Depths of Gramicidin Analogues. It is evident from Figure 2a that the fluorescence

Table 1. Fluorescence Lifetimes of Double Tryptophan Analogues of Gramicidin[a]

gramicidin analogue	α_1	τ_1 (ns)	α_2	τ_2 (ns)	α_3	τ_3 (ns)	τ_m[b] (ns)	$\langle\tau\rangle$[c] (ns)
Phe^{9,11}gA	0.34	0.58	0.42	2.37	0.24	5.56	2.53	3.93
Phe^{13,15}gA	0.32	0.22	0.36	1.89	0.32	4.39	2.18	3.48

[a]The excitation wavelength was 295 nm, and emission was monitored at 340 nm. All other conditions are as in Figure 2. The errors were 5–10% for all parameters. See the Experimental Section for other details. [b]Calculated using eq 3. [c]Calculated using eq 4.

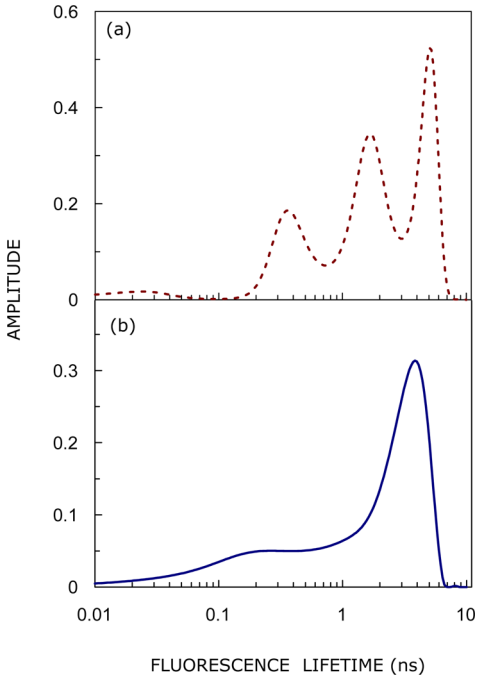

Figure 4. MEM lifetime distribution of tryptophan residues in (a) Phe^{9,11}gA (---) and (b) Phe^{13,15}gA (—) in POPC vesicles. The reduced χ^2 ratios for the distributions are 0.97 and 1.06, respectively. The ratio of peptide to POPC was 1:50 (mol/mol), and the concentration of POPC was 0.85 mM. See the Experimental Section for other details.

emission spectra of the gramicidin analogues are dependent on the positions of tryptophan residues in the sequence. Such a position dependence of the emission maximum could indicate different locations of the tryptophan residues along the membrane axis. The location, depth, orientation, and distribution of the tryptophan residues of gramicidin are different in the channel and nonchannel conformations.[12,17,21,33,36] The distribution of tryptophans along the membrane axis is more extensive in the nonchannel conformation.[7,17,50] Analysis of membrane penetration depths of the gramicidin analogues (Phe^{13,15}gA and Phe^{9,11}gA) containing the inner (Trp-9 and -11) and outer (Trp-13 and -15) tryptophans would therefore provide useful information.

Average depths of the individual tryptophan residues in membrane-bound gramicidin analogues were calculated by the parallax method[51] using the equation

$$z_{cF} = L_{c1} + \{[(-1/\pi C)\ln(F_1/F_2) - L_{21}^2]/2L_{21}\} \quad (9)$$

where z_{cF} = the depth of the fluorophore from the center of the bilayer, L_{c1} = the distance of the center of the bilayer from the shallow quencher (5-PC in this case), L_{21} = the difference in depth between the two quenchers (i.e., the transverse distance between the shallow and the deep quencher), and C = the two-dimensional quencher concentration in the plane of the membrane (molecules/Å^2). Here, F_1/F_2 is the ratio of F_1/F_o and F_2/F_o in which F_1 and F_2 are fluorescence intensities in the presence of the shallow (5-PC) and deep (12-PC) quencher, respectively, both at the same quencher concentration C; F_o is the fluorescence intensity in the absence of any quencher. All bilayer parameters used were the same as described previously.[51] The average depths of penetration of the inner (Trp-9 and -11) and outer (Trp-13 and -15) pair tryptophan residues in Phe^{13,15}gA and Phe^{9,11}gA are shown in Table 2, with

Table 2. Membrane Penetration Depths of the Tryptophan Residues in Gramicidin Analogues by the Parallax Method[a]

gramicidin analogue	distance from the center of the bilayer z_{cF} (Å)
Phe^{9,11}gA	13.9
Phe^{13,15}gA	4.2
gramicidin (channel)[b]	11.0
gramicidin (non-channel)[b]	7.3

[a]Depths were calculated from fluorescence quenchings obtained with samples containing 15 mol % of 5- or 12-PC and using eq 9. Samples were excited at 280 nm, and emission was collected at 335 nm. The ratio of peptide to total lipid was 1:50 (mol/mol). See the Experimental Section for other details. [b]From ref 17.

comparisons to the average depths of the ensemble of four tryptophans of native gramicidin in the channel and non-channel conformations. The inner pair of tryptophans in Phe^{13,15}gA are localized at a relatively deep region in the membrane bilayer, as evidenced from the average depth of 4.2 Å from the center of the bilayer. In contrast, the outer pair of tryptophans in Phe^{9,11}gA are localized at an average depth of 13.9 Å, i.e., at a shallow interfacial region in the membrane. These results are in overall agreement with depths obtained using single tryptophan analogues of gramicidin.[36] The localization of the outer pair of tryptophans is in agreement with the red-shifted emission maximum (338 nm) displayed by the analogue Phe^{9,11}gA compared to an emission maximum of 331 nm exhibited by the analogue Phe^{13,15}gA. Although these are average depths, they are useful, since they represent the lower limit of depth of penetration.

Time-Resolved Anisotropy of Gramicidin Analogues. The information about rotational dynamics is provided by the time-resolved anisotropy of the inner and outer pair of tryptophan residues in double tryptophan gramicidin analogues. Figure 5 shows the time-resolved decay of fluorescence anisotropy of tryptophan residues in Phe^{13,15}gA and Phe^{9,11}gA

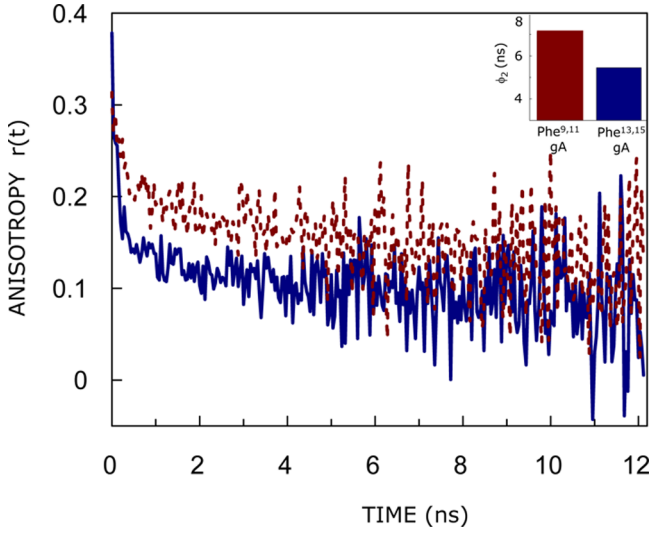

Figure 5. Time-resolved fluorescence anisotropy decay of tryptophan residues in Phe^{13,15}gA (—) and Phe^{9,11}gA (---) in vesicles of POPC. The excitation wavelength was 295 nm, and emission was monitored at 340 nm with a combination of a monochromator and a 320 nm cutoff filter, using a TCSPC setup. The inset shows the relative magnitudes of ϕ_2. The ratio of peptide to POPC was 1:50 (mol/mol), and the concentration of POPC was 0.85 mM. See the Experimental Section for other details.

dx.doi.org/10.1021/jp304846f | J. Phys. Chem. B 2012, 116, 11056−11064

analogues in membranes. As evident from the anisotropy decay, the analogue Phe^{13,15}gA containing the inner pair of tryptophans (Trp-9 and -11) displays faster rotational dynamics compared to the analogue (Phe^{9,11}gA) containing the outer pair of tryptophans (Trp-13 and -15). The anisotropy decay kinetics could be fitted to a sum of three exponentials, and the values of the rotational correlation times (ϕ) are given in Table 3. The

Table 3. Time-Resolved Fluorescence Anisotropy Decay Parameters of Gramicidin Analogues[a]

gramicidin analogue	β_1	ϕ_1 (ns)	β_2	ϕ_2 (ns)	β_3	ϕ_3 (ns)	r_0
Phe^{9,11}gA	0.35	0.39	0.43	7.10	0.23	>200	0.30
Phe^{13,15}gA	0.55	0.30	0.22	5.45	0.23	>200	0.30

[a]All conditions are as in Table 1. The errors were 5−10% for all parameters. See the Experimental Section for other details.

time-resolved anisotropy decay of double tryptophan gramicidin analogues in POPC membranes showed three rotational correlation times: ϕ_1 in the range 0.3−0.5 ns (local motion), ϕ_2 in the range 4−8 ns (segmental motion), and ϕ_3 longer than 200 ns (global motion).[44] The rotational correlation times are in the range of previously reported values of native gramicidin.[17] The lower limit of ϕ_3 comes from our observation window of ∼12 ns, which is dictated by the fluorescence lifetime. The most striking difference is the relatively large amplitude (β_1) associated with the local motion (ϕ_1) displayed by Phe^{13,15}gA containing the inner pair of tryptophans (Figure 5 and Table 3). This result indicates a larger cone angle[52] associated with the motional dynamics of these tryptophans compared to the outer pair of tryptophans in Phe^{9,11}gA and a relatively large degree of motional freedom. This could be due to the intrinsic dynamic gradient of the membrane bilayer[8,46] (see the Discussion). Interestingly, ϕ_2, which represents the segmental motion of tryptophan residues defined by the relative amplitudes, shows a dependence on their localization in the membrane (see Table 3). For example, ϕ_2 for the analogue Phe^{13,15}gA is shorter (5.45 ns, thereby resulting in faster depolarization) than the corresponding rotational correlation time for the analogue Phe^{9,11}gA. It therefore appears that ϕ_2 represents the overall trend among the three rotational correlation times (see Figure 5 and inset).

DISCUSSION

The role of tryptophan residues in the structure and function of membrane proteins and peptides has attracted considerable attention.[9,23,25,26,53,54] It appears that tryptophan residues in integral membrane proteins and peptides are not uniformly distributed yet tend to be localized toward the membrane interface, possibly because they are involved in hydrogen bonding[37,55] with the lipid carbonyl groups or interfacial water molecules. The interfacial region in membranes is characterized by unique motional and dielectric characteristics distinct from both the bulk aqueous phase and the hydrocarbon-like interior of the membrane.[8,46] In model peptides, the experimentally determined interfacial partitioning of tryptophan is highest among the naturally occurring amino acid residues, thereby accounting for its specific interfacial localization in membrane peptides and proteins.[24] Importantly, the role of tryptophan residues in maintaining the structure and function of membrane proteins is exemplified by the fact that substitution or deletion of tryptophans often results in reduction or loss of protein function.[31,32,56] For example, tryptophan substitution affects channel inactivation and gating in the cases of the nicotinic acetylcholine receptor and cardiac sodium channels.[57,58]

Biological membranes exhibit considerable anisotropy along the axis perpendicular to the membrane plane.[8,46] While the center of the bilayer is nearly isotropic, the upper portion is highly ordered.[59] As a result, properties such as polarity, fluidity, segmental motion, ability to form hydrogen bonds, and extent of solvent penetration vary in a depth-dependent manner in the membrane. Such structural and dynamic features of biological membranes result in a quasi-random distribution of amino acids in membrane proteins and peptides, particularly for aromatic amino acids such as tryptophan.[23−26,37]

Gramicidin channels represent an excellent model for exploring physicochemical principles underlying membrane protein structure and function. Previously, it was shown that the substitution of Trp-13 and -15 by Phe allows gramicidin to retain predominantly the single-stranded $\beta^{6.3}$-helical channel

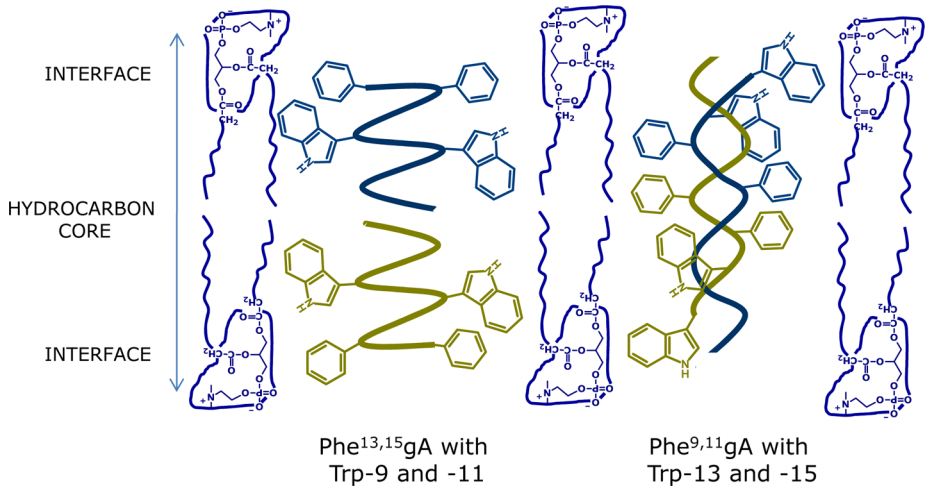

Figure 6. A schematic representation of the effect of pairwise substitution of tryptophan residues of the gramicidin channel. Our results suggest that the double tryptophan gramicidin analogue Phe^{9,11}gA with "outer pair" tryptophan residues (Trp-13 and -15) assumes a conformation which is more nonchannel-like. On the other hand, the analogue Phe^{13,15}gA with an "inner pair" of tryptophans (Trp-9 and -11) assumes a channel-like conformation. See Figure 1 and text for details.

conformation in DMPC bilayers.[38] By contrast, when the more inner Trp-9 and -11 are substituted by Phe, the resulting Phe^{9,11}gA analogue adopts predominantly a double-stranded nonconducting conformation in DMPC. Because DMPC bilayers are relatively thin compared to biological membranes, it was important to investigate the double Phe substituted gramicidin analogues also in the thicker POPC bilayer membranes. In the present work, we confirm in POPC membranes that the substitution of two Trps in a gramicidin subunit by Phe may alter the backbone conformation of membrane-incorporated gramicidin, depending upon the position of the substitutions. The position dependence furthermore remains the same in POPC as in the DMPC bilayer, with the inner tryptophans 9 and 11 being more important for retaining gramicidin's $\beta^{6.3}$-helical channel conformation (see Figure 6).

Analysis of fluorescence data confirms that the inner Trp's (emission maximum 331 nm), in the predominantly channel conformation of gramicidin, are more deeply buried than are the outer Trp's (emission maximum 338 nm), in the predominantly double-stranded gramicidin. The assignments of the conformational preferences in the populations, as deduced in DMPC from CD spectra and size-exclusion chromatograms,[38] are confirmed by the CD spectra of the same analogues in POPC bilayer (Figure 3). The fluorescence lifetimes are furthermore consistent with the conformational preferences, as retaining the inner tryptophans in the analogue (Phe^{13,15}gA) maintains a relatively homogeneous lifetime distribution (Figure 4b). By contrast, when the inner tryptophans are replaced, in the analogue (Phe^{9,11}gA), not only do double-stranded conformations become preferred but also the lifetime distribution becomes more heterogeneous (Figure 4a). The different biophysical measurements show internal consistency for the inner-pair and outer-pair isomeric peptides. Interestingly, the deduced membrane penetration depths differ in a predictable fashion, when the inner pair and outer pair of tryptophans are substituted with phenylalanines. The difference (~10 Å) is furthermore much greater than would be expected for solely changing the Trp sequence positions on a constant backbone helix, again confirming a change in the preferred (predominant) conformation when the inner Trp's are changed to Phe. Taken together, these results are in agrement with the previous structural characterization in DMPC and functional characterization in diphytanoyl-PC of the inner-pair and outer-pair Trp → Phe gramicidin channel analogues.[38] To this picture, the fluorescence measurements add specific information about the tryptophan locations and dynamics in POPC membranes.

We and others have previously shown that single tryptophan gramicidin analogues adopt predominantly nonchannel conformations.[35,36] Our present fluorescence results, together with the recent NMR and single-channel results,[38] show that the positions of tryptophan residues in membranes are important determinants for gramicidin structure and function. In a broader perspective, our results could be potentially useful in analyzing the effects of tryptophan substitution on the function of other ion channels and membrane proteins.

AUTHOR INFORMATION

Corresponding Author

*Phone: +91-40-2719-2578. Fax: +91-40-2716-0311. E-mail: amit@ccmb.res.in.

Notes

The authors declare no competing financial interest.

ACKNOWLEDGMENTS

This work was supported by research grants from the Council of Scientific and Industrial Research (A.C.) and Department of Atomic Energy (G.K.), Govt. of India., and NIH grant GM70971 to R.E.K. The peptide facility was supported by NIH grants GM103429 and GM103450 and by the Arkansas Biosciences Institute. S.H. and Ar.C. thank the Council of Scientific and Industrial Research for the award of Senior Research Fellowships. A.C. is an Adjunct Professor at the Special Centre for Molecular Medicine of Jawaharlal Nehru University (New Delhi, India) and Indian Institute of Science Education and Research (Mohali, India) and Honorary Professor at the Jawaharlal Nehru Centre for Advanced Scientific Research (Bangalore, India). A.C. and G.K. gratefully acknowledge the J.C. Bose Fellowship (Department of Science and Technology, Govt. of India). We thank Prof. N. Periasamy (TIFR, Mumbai) for providing the software for the analysis of MEM data. We thank members of A.C.'s research group for critically reading the manuscript.

REFERENCES

(1) Granseth, E.; Seppälä, S.; Rapp, M.; Daley, D. O.; von Heijne, G. *Mol. Membr. Biol.* **2007**, *24*, 329−332.
(2) Fagerberg, L.; Jonasson, K.; von Heijne, G.; Uhlén, M.; Berglund., L. *Proteomics* **2010**, *10*, 1141−1149.
(3) Drews, J. *Science* **2000**, *287*, 1960−1964.
(4) Dailey, M. M.; Hait, C.; Holt, P. A.; Maguire, J. M.; Meier, J. B.; Miller, M. C.; Petraccone, L.; Trent, J. O. *Exp. Mol. Pathol.* **2009**, *86*, 141−150.
(5) Anson, L. *Nature* **2009**, *459*, 343.
(6) (a) Raghuraman, H.; Chattopadhyay, A. *Langmuir* **2003**, *19*, 10332−10341. (b) Chattopadhyay, A.; Raghuraman, H. *Curr. Sci.* **2004**, *87*, 175−180.
(7) Haldar, S.; Kombrabail, M.; Krishnamoorthy, G.; Chattopadhyay, A. *J. Fluoresc.* **2010**, *20*, 407−413.
(8) Haldar, S.; Chaudhuri, A.; Chattopadhyay, A. *J. Phys. Chem. B* **2011**, *115*, 5693−5706.
(9) Raghuraman, H.; Kelkar, D. A.; Chattopadhyay, A. In *Reviews in Fluorescence 2005*; Geddes, C. D., Lakowicz, J. R., Eds.; Springer: New York, 2005; pp 199−222.
(10) Schiffer, M.; Chang, C. H.; Stevens, F. J. *Protein Eng.* **1992**, *5*, 213−214.
(11) Koeppe, R. E.; Andersen, O. S. *Annu. Rev. Biophys. Biomol. Struct.* **1996**, *25*, 231−258.
(12) Kelkar, D. A.; Chattopadhyay, A. *Biochim. Biophys. Acta* **2007**, *1768*, 2011−2025.
(13) Andersen, O. S.; Koeppe, R. E. *Annu. Rev. Biophys. Biomol. Struct.* **2007**, *36*, 107−130.
(14) Andersen, O. S.; Saberwal, G.; Greathouse, D. V.; Koeppe, R. E. *Ind. J. Biochem. Biophys.* **1996**, *33*, 331−342.
(15) Chattopadhyay, A.; Kelkar, D. A. *J. Biosci.* **2005**, *30*, 147−149.
(16) Townsley, L. E.; Tucker, W. A.; Sham, S.; Hinton, J. F. *Biochemistry* **2001**, *40*, 11676−11686.
(17) Rawat, S. S.; Kelkar, D. A.; Chattopadhyay, A. *Biophys. J.* **2004**, *87*, 831−843.
(18) Kelkar, D. A.; Chattopadhyay, A. *Biophys. J.* **2005**, *88*, 1070−1080.
(19) Rawat, S. S.; Kelkar, D. A.; Chattopadhyay, A. *Biophys. J.* **2005**, *89*, 3049−3058.
(20) O'Connell, A. M.; Koeppe, R. E.; Andersen, O. S. *Science* **1990**, *250*, 1256−1259.
(21) Ketchem, R. R.; Hu, W.; Cross, T. A. *Science* **1993**, *261*, 1457−1460.

(22) Mukherjee, S.; Chattopadhyay, A. *Biochemistry* **1994**, *33*, 5089−5097.
(23) Kelkar, D. A.; Chattopadhyay, A. *J. Biosci.* **2006**, *31*, 297−302.
(24) Wimley, W. C.; White, S. H. *Nat. Struct. Biol.* **1996**, *3*, 842−848.
(25) Andersen, O. S. *J. Gen. Physiol.* **2007**, *129*, 351−352.
(26) Koeppe, R. E. *J. Gen. Physiol.* **2007**, *130*, 223−224.
(27) Sychev, S. V.; Barsukov, L. I.; Ivanov, V. T. *Eur. Biophys. J.* **1993**, *22*, 279−288.
(28) Zein, M.; Winter, R. *Phys. Chem. Chem. Phys.* **2000**, *2*, 4545−4551.
(29) Kelkar, D. A.; Chattopadhyay, A. *Biochim. Biophys. Acta* **2007**, *1768*, 1103−1113.
(30) Daumas, P.; Heitz, F.; Ranjalahy-Rasoloarijao, L.; Lazaro, R. *Biochimie* **1989**, *71*, 77−81.
(31) Becker, M. D.; Greathouse, D. V.; Koeppe, R. E.; Andersen, O. S. *Biochemistry* **1991**, *30*, 8830−8839.
(32) Fonseca, V.; Daumas, P.; Ranjalahy-Rasoloarijao, L.; Heitz, F.; Lazaro, R.; Trudelle, Y.; Andersen, O. S. *Biochemistry* **1992**, *31*, 5340−5350.
(33) Hu, W.; Lee, K.-C.; Cross., T. A. *Biochemistry* **1993**, *32*, 7035−7047.
(34) Andersen, O. S.; Greathouse, D. V.; Providence, L. L.; Becker, M. D.; Koeppe., R. E. *J. Am. Chem. Soc.* **1998**, *120*, 5142−5146.
(35) Salom, D.; Pérez-Payá, E.; Pascal, J.; Abad, C. *Biochemistry* **1998**, *37*, 14279−14291.
(36) Chattopadhyay, A.; Rawat, S. S.; Greathouse, D. V.; Kelkar, D. A.; Koeppe, R. E. *Biophys. J.* **2008**, *95*, 166−175.
(37) Sun, H.; Greathouse, D. V.; Andersen, O. S.; Koeppe., R. E. *J. Biol. Chem.* **2008**, *283*, 22233−22243.
(38) Gu., H.; Lum, K.; Kim, J. H.; Greathouse, D. V.; Andersen, O. S.; Koeppe, R. E. *Biochemistry* **2011**, *50*, 4855−4866.
(39) Baron, C. B.; Coburn, R. F. *J. Liq. Chromatogr.* **1984**, *7*, 2793−2801.
(40) McClare, C. W. F. *Anal. Biochem.* **1971**, *39*, 527−530.
(41) Abrams, F. S.; London., E. *Biochemistry* **1993**, *32*, 10826−10831.
(42) Lakowicz, J. R. *Principles of Fluorescence Spectroscopy*, 3rd ed.; Springer: New York, 2006.
(43) Valeur, B. *Molecular Fluorescence*; Wiley-VCH: Weinheim, Germany, 2002.
(44) Mukherjee, S.; Kombrabail, M.; Krishnamoorthy, G.; Chattopadhyay, A. *Biochim. Biophys. Acta* **2007**, *1768*, 2130−2144.
(45) Paila, Y. D.; Kombrabail, M.; Krishnamoorthy, G.; Chattopadhyay, A. *J. Phys. Chem. B* **2011**, *115*, 11439−11447.
(46) Chattopadhyay, A. *Chem. Phys. Lipids* **2003**, *122*, 3−17.
(47) Demchenko, A. P. *Methods Enzymol.* **2008**, *450*, 59−78.
(48) Prendergast, F. G. *Curr. Opin. Struct. Biol.* **1991**, *1*, 1054−1059.
(49) Krishnamoorthy, G.; Ira. *J. Fluoresc.* **2001**, *11*, 247−253.
(50) Arumugam, S.; Pascal, S.; North, C. L.; Hu, W.; Lee, K.-C.; Cotten, M.; Ketchem, R. R.; Xu, F.; Brenneman, M.; Kovacs, F.; et al. *Proc. Natl. Acad. Sci. U.S.A.* **1996**, *93*, 5872−5876.
(51) Chattopadhyay, A.; London, E. *Biochemistry* **1987**, *26*, 39−45.
(52) Kinosita, K. J.; Kawato, S.; Ikegami, A. *Biophys. J.* **1977**, *20*, 289−305.
(53) Reithmeier, R. A. F. *Curr. Opin. Struct. Biol.* **1995**, *5*, 491−500.
(54) Chattopadhyay, A.; Mukherjee, S.; Rukmini, R.; Rawat, S. S.; Sudha., S. *Biophys. J.* **1997**, *73*, 839−849.
(55) Ippolito, J. A.; Alexander, R. S.; Christianson, D. W. *J. Mol. Biol.* **1990**, *215*, 457−471.
(56) Miller, A. S.; Falke., J. J. *Biochemistry* **2004**, *43*, 1763−1770.
(57) Lasalde, J. A.; Tamamizu, S.; Butler, D. H.; Vibat, C. R.; Hung, B.; McNamee., M. G. *Biochemistry* **1996**, *35*, 14139−14148.
(58) Wang, S. Y.; Russell, C.; Wang, G. K. *Biophys. J.* **2005**, *88*, 3991−3999.
(59) Chattopadhyay, A.; Mukherjee., S. *Langmuir* **1999**, *15*, 2142−2148.